Excitations in the Ordered and Paramagnetic States of Honeycomb Magnet $Na_2Co_2TeO_6$

Weiliang Yao,[1,*,†] Kazuki Iida,[2] Kazuya Kamazawa,[2] and Yuan Li[1,3,‡]
[1]International Center for Quantum Materials, School of Physics, Peking University, Beijing 100871, China
[2]Neutron Science and Technology Center, Comprehensive Research Organization for Science and Society, Tokai, Ibaraki 319-1106, Japan
[3]Collaborative Innovation Center of Quantum Matter, Beijing 100871, China

(Received 8 March 2022; accepted 13 September 2022; published 30 September 2022)

$Na_2Co_2TeO_6$ is a proposed approximate Kitaev magnet, yet its actual magnetic interactions are elusive due to a lack of knowledge on the full excitation spectrum. Here, using inelastic neutron scattering and single crystals, we determine the system's temperature-dependent magnetic excitations over the entire Brillouin zone. Without committing to specific models, we unveil a distinct signature of the third-nearest-neighbor coupling in the spin waves, which signifies the associated distance as an emerging effective link in the ordered state. The presence of at least six nonoverlapping spin-wave branches is at odds with all models proposed to date. Above the ordering temperature, persisting dynamic correlations can be described by equal-time magnetic structure factors of a hexagonal cluster, which reveal the leading instabilities. Our result sets definitive constraints on theoretical models for $Na_2Co_2TeO_6$ and provides new insight for the materialization of the Kitaev model.

DOI: 10.1103/PhysRevLett.129.147202

A quantum spin liquid (QSL) is a novel state of matter where localized spins defy formation of long-range order due to frustrated interactions and/or quantum fluctuations [1–3]. The concept has stimulated intense research ever since the original proposal of resonating valence bonds by Anderson [4]. In recent years, the spin-1/2 Kitaev honeycomb model has become another booming direction to search for QSLs [5–8]. In this model, spins with bond-dependent Ising interactions (Kitaev interactions) are highly frustrated, and they form QSL ground states along with fractionalized excitations [9].

Materialization of the Kitaev model is illuminated by a mechanism proposed by Jackeli and Khaliullin [10] in Mott insulators with strong spin-orbit coupling (SOC). α-$RuCl_3$ and Na_2IrO_3 are two representative candidates, where the Ru^{3+} and Ir^{4+} ions have a low-spin d^5 electronic configuration and an atomic ground state of a spin-orbit entangled Kramers doublet [11–13]. The edge-sharing $RuCl_6$ and IrO_6 octahedra form layered honeycomb lattices, which host nearest-neighbor Kitaev interactions [10]. Even though neither system has a QSL ground state under ambient conditions, experiments have suggested a major role of Kitaev interactions in the magnetic models [6,14–17], whereas the deviation from QSL states is attributed to the presence of additional non-nearest-neighbor-Kitaev terms [18–20]. Moreover, evidence for a QSL state has been reported in α-$RuCl_3$ under in-plane magnetic fields [21–25], which have become widely used for the search of QSLs in putative Kitaev magnets with long-range order.

Furthering the Jackeli-Khaliullin mechanism, recent theoretical studies indicate that Kitaev interactions can arise between $3d$ transition-metal ions with a high-spin d^7 electronic configuration ($t_{2g}^5 e_g^2$) [26–31]. While both Co^{2+} and Ni^{3+} ions can serve for this purpose [29], materials studied so far are mostly Co based, because Ni^{3+} is an uncommon oxidation state in solids. Co-based candidate Kitaev magnets include $Na_2Co_2TeO_6$ [32–35], $A_3Co_2SbO_6$ (with A = Li, Na, and Ag) [32,36–39], $CoTiO_3$ [40,41], $BaCo_2(AsO_4)_2$ [42,43], and $BaCo_2(PO_4)_2$ [44]. Although all of them develop long-range order at low temperatures, the ordering can be suppressed by in-plane fields in $Na_2Co_2TeO_6$ [45,46] and $BaCo_2(AsO_4)_2$ [43], similar to the behavior of α-$RuCl_3$. Their thermal transport properties are also similar to α-$RuCl_3$ [43,47].

With these promising properties, $Na_2Co_2TeO_6$ has recently been intensively studied [45,46,48–52]. A widely recognized goal is to establish the magnetic interaction model with inelastic neutron scattering (INS) [46,48,50–52], yet most of the experiments so far were performed on powder samples and pointed to diversifying sets of parameters. In this Letter, we report extensive INS data taken on high-quality single crystals, which enable us to map out magnetic excitations over the two-dimensional (2D) Brillouin zone and study their temperature dependence in conjunction with thermodynamics. We find that a third-nearest-neighbor interaction alone provides a highly accurate effective description of the low-energy spin waves, whereas the full spin-wave spectrum is at variance with all presently available models. Moreover, the paramagnetic state features persisting short-range magnetic correlations accountable by zigzag-type magnetization on a hexagonal cluster. These results provide new insights on the closely

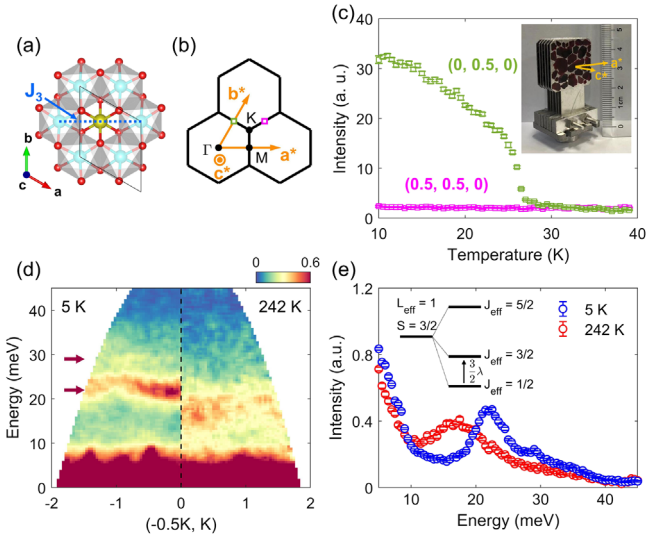

FIG. 1. (a) A honeycomb layer of $Na_2Co_2TeO_6$. Cyan, yellow, and red spheres represent Co, Te, and O, respectively. Solid lines indicate a 2D primitive cell. Dotted line connects a pair of third-nearest-neighbor Co^{2+} ions. The illustration is produced with VESTA [54]. (b) 2D reciprocal space and hexagonal Brillouin zones. (c) Diffraction at (0, 0.5, 0) and (0.5, 0.5, 0), measured versus T with $E_i = 10.0$ meV. The two $\mathbf{Q}$ positions are indicated in (b). Inset shows a photograph of our sample. (d) Crystal-field excitations along $\mathbf{Q}_{2D} = (-0.5K, K)$, measured at two temperatures with $E_i = 52.9$ meV. (e) Energy distribution of intensity, after integrating the (symmetrized) data in (d) over $K \in [-1, 1]$. Inset illustrates the splitting of the 12-fold degenerate atomic $L_{\text{eff}} = 1$, $S = 3/2$ states under the influence of SOC. Arrow indicates the observed excitations in the fully localized limit.

competing interactions and instabilities in $Na_2Co_2TeO_6$, paving the way to a deeper understanding of Kitaev magnets.

$Na_2Co_2TeO_6$ has nearly ideal honeycomb layers of edge-sharing CoO_6 octahedra [Fig. 1(a)] [32–35]. As the deviation from an ideal octahedral crystal field is small compared to the SOC energy, the Co^{2+} ions in their high-spin configuration are expected to have a pseudospin $J_{\text{eff}} = 1/2$ ground state [26,27]. Below $T_N \sim 26.5$ K, the system develops long-range three-dimensional antiferromagnetic (AFM) order with a propagation vector (0, 1/2, 0) and its symmetry-related equivalents [34,35,50]. The precise magnetic structure, however, has some ambiguities: one possibility is a zigzag structure [33,34,50], which has C_3-related domains in a macroscopic sample; another is a "triple-$\mathbf{q}$" structure formed by the vector sum of all C_3-related zigzag structures [49], which was originally discussed as a field-induced state [53]. Difficult to distinguish in most experiments, these two structures are both referred to as zigzag type in the present study.

Single crystals of $Na_2Co_2TeO_6$ were grown by a modified flux method described in [55]. About 200 crystals (~2 g in total) were coaligned within ~2° with reciprocal vectors $\mathbf{a}^*$ and $\mathbf{c}^*$ horizontal [Figs. 1(b) and 1(c) inset]. The INS experiment was performed on the 4SEASONS time-of-flight spectrometer at the MLF, J-PARC, Japan [58], using a main incident neutron energy $E_i = 10.0$ meV and Fermi chopper frequency 150 Hz. Data from additional E_i's (2.9, 4.1, 6.1, 19.4, and 52.9 meV) were obtained simultaneously [59]. Sample-rotation ("4D") measurements were performed at nine temperatures ($T = 5$, 14, 21, 28, 35, 63, 120, 242, and 290 K). Data were analyzed with UTSUSEMI [60], HORACE [61], and DAVE [62]. All intensities except for those obtained with $E_i = 52.9$ meV were converted to absolute units [63] using phonon scattering around (3, 0, 0) [55]. To present excitations in the (H, K) plane, the normalized data were averaged over the entire covered L range. Spin-wave calculations were performed with SpinW [64]. Specific heat measurements were performed on a single crystal with the Quantum Design PPMS, where the magnetic specific heat was obtained by subtracting lattice contributions measured on a nonmagnetic $Na_2Zn_2TeO_6$ reference crystal [45].

Since variations of ordering temperatures caused by sample imperfection have greatly complicated the interpretation of results in α-$RuCl_3$ [14,65], a precheck of the magnetic ordering in our $Na_2Co_2TeO_6$ crystal array is desired. Figure 1(c) presents the T dependence of a magnetic Bragg peak at (0, 0.5, 0). The observed transition around 26.5 K is consistent with thermodynamically determined T_N [34,35], confirming the high homogeneity of our sample. No temperature dependence is found for the intensity at (0.5, 0.5, 0), which rules out the so-called stripe-type magnetic order [66].

Given the relatively weak SOC in 3d transition metals, the pseudospin picture is not necessarily adequate for describing the low-energy physics in Co-based compounds [30,67]. To check this, we inspect the crystal-field excitations of $Na_2Co_2TeO_6$. As presented in Figs. 1(d) and 1(e), *two* excitation levels can be observed between 20 and 30 meV at 5 K. The more pronounced one around 22 meV has clear dispersion along $(-0.5K, K)$, and its intensity distribution in the (H, K) plane can be found in [55]. Well above T_N, the excitations move to lower energy due to vanishing molecular fields associated with the long-range magnetic order, which can be more clearly seen from the energy distribution plot in Fig. 1(e). A zeroth-order approximation to these excitations is the process of exciting electrons from $J_{\text{eff}} = 1/2$ to $J_{\text{eff}} = 3/2$ states [30,48,67], schematically showed in the inset of Fig. 1(e). Hence, the persistence of the excitations to far above T_N supports the validity of the $J_{\text{eff}} = 1/2$ picture (see Ref. [55] for detailed discussions). The nonzero dispersion of the 22 meV band, and the presence of a weaker high-energy sideband close to 30 meV at 5 K, are likely due to non-negligible electron hopping between neighboring sites and intermixing between the $J_{\text{eff}} = 1/2$ and 3/2 states [68] under additional nonoctahedral crystal fields.

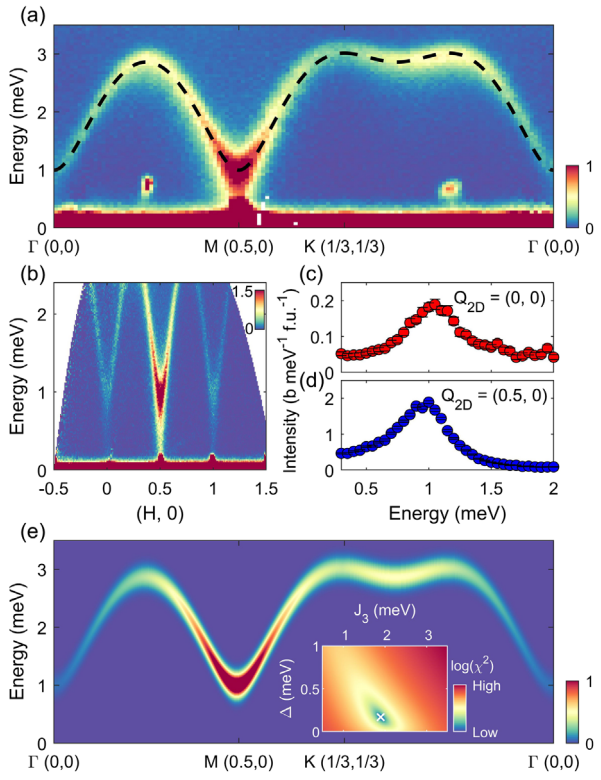

FIG. 2. (a) Low-energy spin waves along high-symmetric lines of the Brillouin zone [Fig. 1(b)], measured with $E_i = 6.1$ meV. Two singular signals below 1 meV are artifacts (multiple scattering). Dotted line is a fit dispersion, see text. (b) Band bottoms of spin waves along $(H, 0)$, measured with $E_i = 2.9$ meV. (c),(d) Energy cuts at (0, 0) and (0.5, 0), based on the same data as in (b). Slight difference in the peak-maximum energy is due to resolution effects. (e) Calculated spin waves using the model in Eq. (1) for comparison to (a). Inset shows the goodness of fit (χ^2) versus J_3 and Δ. White cross indicates the best-fit parameters used for the main panel. For details of the fitting, see Ref. [55].

Next, we turn to magnetic excitations within the $J_{\text{eff}} = 1/2$ manifold. Figure 2(a) presents the lowest-energy spin wave branch along high-symmetric lines in the 2D Brillouin zone. This branch reaches the same energy minimum (∼1 meV) at both the M and Γ points [Figs. 2(b)–2(d)]. While similar energies were reported previously [46,48,50–52], the powder INS studies could not unambiguously compare the M and Γ points. Importantly, if a zigzag ground state were driven by Kitaev interactions, the spin waves would reach their band minimum at the M point, and become higher-energy flat modes near the Γ point [14,18], different from our observation. The data in Fig. 2 therefore support either a zigzag structure driven primarily by competing Heisenberg terms ([46], Fig. S7b in [55]) or a triple-**q** magnetic structure [49].

Local-moment models usually have prominent nearest-neighbor interactions, as has also been inferred from powder INS data [46,48,50–52]. Surprisingly, the lowest-energy spin waves can be adequately described by an effective model with *only* third-nearest-neighbor AFM coupling (J_3) and gap-opening anisotropy (Δ) terms:

$$H = J_3 \sum_{\langle\langle\langle i,j \rangle\rangle\rangle} \mathbf{S}_i \cdot \mathbf{S}_j - \Delta \sum_i (\mathbf{S}_i \cdot \hat{n}_i)^2. \quad (1)$$

The model has Néel order on each of the four J_3-linked (enlarged honeycomb) sublattices, and $\hat{n}_i$ denotes the ordered spin direction at site i. The model's best-fit parameters [Fig. 2(e), inset] after the observed dispersion in Fig. 2(a), $J_3 = 1.896(9)$ meV and $\Delta = 0.170(6)$ meV, also reproduce the observed intensities very well [Fig. 2(e)]. We attribute the success of this model to an emerging network of J_3 in the AFM ordered state, and make three remarks: (1) We have explored adding nearer-neighbor couplings (J_1 and J_2) and calculating spin waves from a zigzag structure, but they do not improve the fit, which always converges to a J_3-dominant case, see Fig. S6 in [55] for detail. (2) The J_3-Δ model is compatible with all zigzag-type structures as they are degenerate ground states. In the limit that the inter-sub-lattice interactions are cancelled in the ordered structure, the low-energy dynamics will be dictated by the effective J_3 and Δ. (3) Taking a metaphor to a crystal of organic molecules: the lowest-energy phonons will reflect the weak intermolecular coupling (e.g., hydrogen bonds and van der Waals forces), rather than the strong intramolecular coupling (e.g., covalent bonds). Similarly, without knowing the bare exchange interactions, J_3 in our model could be an effective coupling that derives from the bare interactions under a frustrated order, which features small magnetic clusters linked by the effective J_3.

At higher energy up to 12 meV, we observe at least five weakly dispersing excitation branches [Fig. 3(a)]. We attribute them to additional spin waves, because they completely disappear above T_N [Fig. 3(b)] and have a rich variety of dynamic structure factors at 5 K [Figs. 3(c)–3(h)]. The factor of ∼2 energy hierarchy compared to the crystal-field levels provides an estimate of how good the $J_{\text{eff}} = 1/2$ description is at such low temperatures, where thermal excitation to the $J_{\text{eff}} = 3/2$ states is negligible. By applying a sum-rule analysis [55,63,69], we obtain a total spectral weight (from 1 meV to 14 meV) corresponding to $g^2 S \approx 7.53$ at 5 K. The inferred g factor (for simplicity, assumed to be a scalar) of ∼4 for effective $S = 1/2$ is consistent with electron paramagnetic resonance measurements [46]. We consider a complete model for the spin waves out of reach at present, in part due to the unknown magnetic structure. Our separate explorations of the possible zigzag and triple-**q** structures reveal further difficulty: the former is found to require fine-tuning in order for a multidomain sample to produce seemingly nonoverlapping (see below) spin waves, whereas the latter's stability may require new mechanisms beyond common considerations [20,70,71]. Certain conditions are known to enforce a degeneracy between the two structures [72], where further theoretical

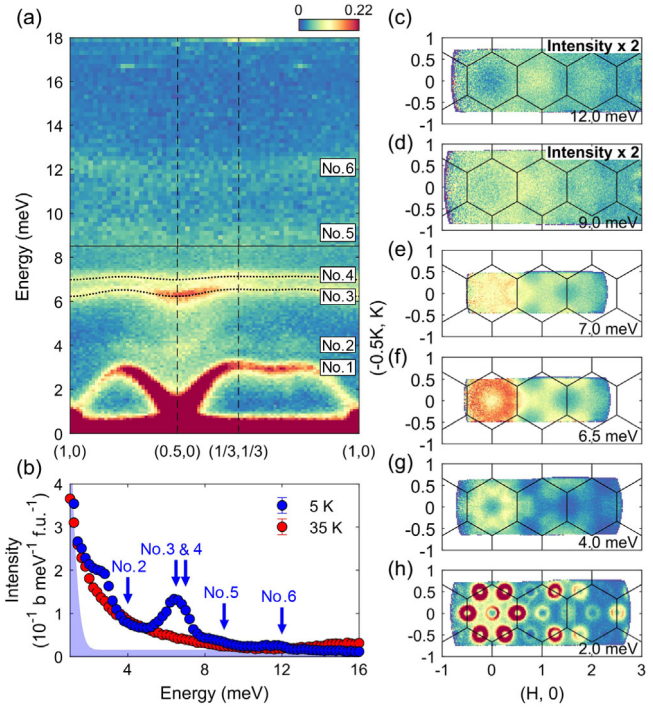

FIG. 3. (a) At least six spin-wave branches are observed at 5 K. Data are measured with $E_i = 10.0$ meV (lower part) and 19.4 meV (upper part). Dotted curves indicate fit dispersions [55]. (b) Brillouin-zone averaged intensity versus energy, measured with $E_i = 19.4$ meV. Shaded area indicates background scattering (excluded from the sum-rule analysis discussed in the text). The slightly increased intensity above 12 meV at 35 K is contributed by the softened crystal field excitations (Fig. 1). (c)–(h) Spin-wave signals at selected energies.

progress might allow for a systematic optimization of the spin waves. We note a few key characteristics in Fig. 3: (i) The lowest-energy branch carries most of the spectral weight and thus dominates the dynamic correlations. (ii) The next most pronounced branches, No. 3 and No. 4 in Fig. 3(b), have qualitatively similar dispersion and $S(\mathbf{Q})$ as the lowest branch [Fig. 3(a)]. In Fig. S5 in [55], we show that they can also be described by variations of the J_3-Δ model, which further signifies the important role of the third-nearest-neighbor coupling in the spin-wave propagation. (iii) The number of spin-wave branches sets a lower bound on the number of spins in the magnetic primitive cell. The branches have no overlap, which is distinct from other honeycomb magnets with branch crossings [41,66,73,74]. This further hints at the existence of magnetic clusters [75] in the ordered state.

We have compared our experimental data to spin waves calculated from published models (see Ref. [55] for the actual comparisons), and found all of them to be at variance with our INS data, especially concerning characteristic (iii) above. Once averaged over sample orientations (Fig. S5 in [55]), our data are fully consistent with powder INS spectra [46,48,50–52], including having a concave E-Q envelope shape at small Q near the M point, which has been taken as a key indication for zigzag order in α-$RuCl_3$ and Na_2IrO_3 [6,14,66]. We believe that further theoretical work is needed to coherently account for the elusive magnetic ground state, the multiple thermal [45,49] and field-induced transitions [45,46], and the spin waves in $Na_2Co_2TeO_6$. Our extensive INS data provide a solid ground for such explorations.

The physical essence of our effective J_3 may be important. The inclusion of J_3 on the honeycomb lattice is known to produce rich competing phases in models both with [19,20,76–78] and without [70,79] anisotropic (e.g., Kitaev) terms. In particular, a classical-energy degeneracy between collinear and noncollinear zigzag-type states is found in the Heisenberg models [79]. From a structural point of view, the Co hexagons in $Na_2Co_2TeO_6$ are centered around Te atoms, whose spatially extended d orbitals may promote electron hopping and further-neighbor coupling. Even in the cases of α-$RuCl_3$ and Na_2IrO_3, which have no or small-ionic-radius atoms at the hexagon centers, the role of itinerancy [80,81] and further-neighbor coupling [82–84] has been actively discussed in recent years.

We last discuss magnetic correlations in the paramagnetic state. They manifest themselves in the INS spectra as an energy down-flow of spin-wave signals from the ordered state [Fig. 4(a)]. The persistence of finite-energy dynamics to far above T_N is in line with the presence of appreciable magnetic specific heat above T_N [Fig. 4(b)]. These behaviors resemble α-$RuCl_3$, where interpretations have been made around thermodynamics of Majorana fermions [7,85]. We refrain from making related speculations here, since the microscopic model is unclear at present (which may support short-range correlations [86,87] rather than fractional excitations above T_N), and because Co^{2+} electronic excitations beyond the $J_{\text{eff}} = 1/2$ manifold also contribute specific heat at high T, making the total entropy there exceed $2R \ln 2$ [Fig. 4(b)]. Figures 4(c) and 4(d) show that the paramagnetic fluctuations are weakly structured in energy, but strongly structured in $\mathbf{Q}$: intensities are concentrated around the M points, indicative of instability towards the ordering at low T. The $\mathbf{Q}$-space structure does not vary strongly with increasing T, only the overall intensity decreases [Fig. 4(a)]. After a widely used method for analyzing frustrated magnets [88–92], we model the $\mathbf{Q}$ dependence with equal-time spin correlations, by considering scattering interference from a hexagonal unit:

$$I(\mathbf{Q}) = f^2(\mathbf{Q}) \sum_{m,n} e^{i\mathbf{Q}\cdot(\mathbf{r}_m - \mathbf{r}_n)} \sum_{\alpha,\beta} \left(\delta_{\alpha,\beta} - \frac{Q_\alpha Q_\beta}{Q^2} \right) \langle S_m^\alpha S_n^\beta \rangle, \tag{2}$$

where $f(\mathbf{Q})$ is the magnetic form factor of Co^{2+}, S_m^α, and S_n^β are spin components α and β at sites $\mathbf{r}_m$ and $\mathbf{r}_n$, respectively, with $m, n \in \{1, \ldots, 6\}$, $\alpha, \beta \in \{x, y, z\}$ and

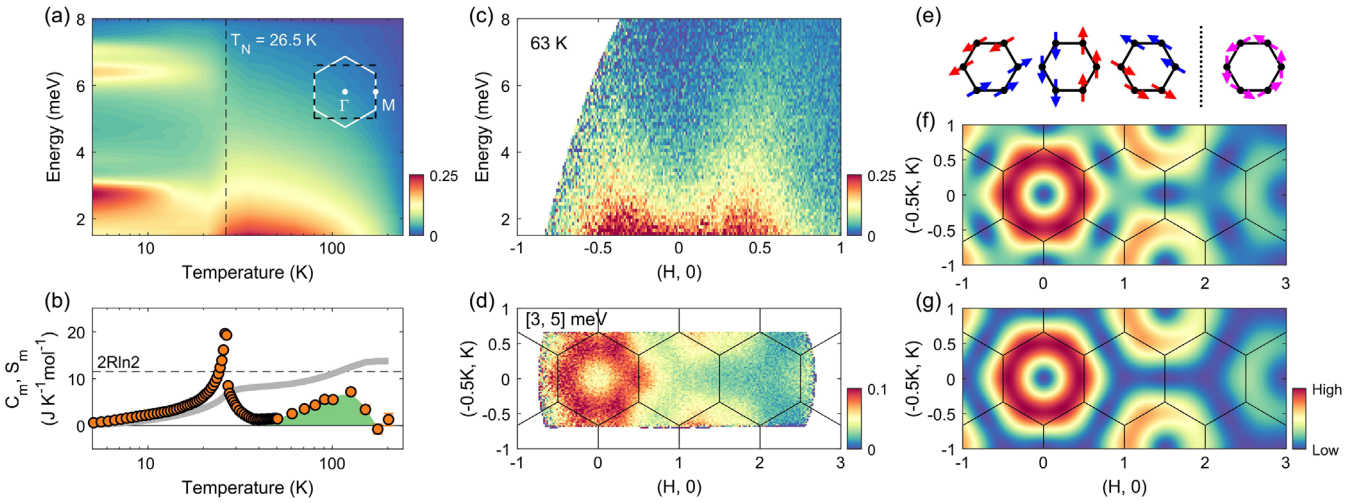

FIG. 4. (a) Energy and temperature dependence of intensity averaged over a Brillouin zone (dashed black rectangle in inset), based on data obtained at eight temperatures with $E_i = 10.0$ meV, after subtraction against $T = 290$ K as background. (b) Magnetic specific heat (dots) and entropy (gray line). Shaded area indicates entropy release above T_N. (c),(d) Paramagnetic fluctuations measured with $E_i = 10.0$ meV at 63 K. (e) Local zigzag arrangements on a hexagonal unit (left), and their vector superposition forming a vortexlike pattern (right). (f),(g) Calculated $I(\mathbf{Q})$ (see text) for the two arrangements in (e).

$\delta_{\alpha,\beta} - Q_\alpha Q_\beta / Q^2$ being a projection factor for unpolarized neutron scattering. $\langle \cdots \rangle$ assumes a 4π (global) rotational average of all six spins in the paramagnetic state. For two zigzag-type arrangements depicted in Fig. 4(e), the above formula can be further simplified as

$$I(\mathbf{Q}) = \frac{3}{4} f^2(\mathbf{Q}) \left\langle \left| \sum_{m=1,\ldots,6} S e^{i(\phi_m + \mathbf{Q}\cdot\mathbf{r}_m)} \right|^2 \right\rangle_{\text{eq}}, \qquad (3)$$

where S is the spin size and ϕ_m the angle in the honeycomb plane at site m, and $\langle \cdots \rangle_{\text{eq}}$ averages over symmetry equivalents [on the left of Fig. 4(e)].

Using the collinear and noncollinear zigzag-type clusters [Fig. 4(e)], the calculated $I(\mathbf{Q})$ are displayed in Figs. 4(f) and 4(g), respectively, which agree nicely with the measurement data. Simulations of other spin arrangements on a hexagon can be found in [55]. We therefore conclude that the paramagnetic fluctuations are adequately described within one hexagonal unit, and that they are essentially zigzag-type AFM fragments. A common characteristic of the two arrangements in Fig. 4(e) is that the (presumably AFM) J_3 coupling always connects opposite spins, reminding us of J_3's fingerprint on the most pronounced spin waves in the ordered state. Last but not the least, the vortexlike arrangement in Fig. 4(e) can be understood as a nonzero local expected value of the hexagon-flux operator W_p [6,9]. Since W_p is a local Z_2 conserved quantity of the Kitaev model, the paramagnetic fluctuations might have a deep implication on the QSL physics.

In conclusion, we have successfully mapped out the magnetic excitations in $Na_2Co_2TeO_6$ single crystals. Low-energy dynamics in both the ordered and the thermally disordered states show a strong indication of magnetic coupling between third-nearest neighbors. While the results do not necessarily mean that J_3 is a leading interaction, they do suggest the emergence of magnetic clusters featuring the third-nearest distance. Since $Na_2Co_2TeO_6$ shares important thermodynamic and spectroscopic characteristics with previous Kitaev-like magnets, we expect our result to stimulate new thinking of Kitaev materials in general, especially in conjunction with structural properties and electron itinerancy.

We wish to thank Cristian Batista, Wenjie Chen, V. Ovidiu Garlea, Christian Hess, Xiaochen Hong, Lukas Janssen, Chaebin Kim, Wilhelm G. F. Krüger, Ke Liu, Zhengxin Liu, Je-Geun Park, Fa Wang, and Jiucai Wang for discussions. Work at Peking University was supported by the National Basic Research Program of China (Grant No. 2018YFA0305602) and the NSF of China (Grants No. 11874069, No. 12061131004, No. 11888101). The INS experiment was performed at the MLF, J-PARC, Japan, under a user program (Proposal No. 2019B0062).

*wyao4@utk.edu
†Present address: Department of Physics, University of Tennessee, Knoxville, Tennessee 37996, USA.
‡yuan.li@pku.edu.cn

[1] L. Balents, Nature (London) **464**, 199 (2010).
[2] Y. Zhou, K. Kanoda, and T.-K. Ng, Rev. Mod. Phys. **89**, 025003 (2017).
[3] C. Broholm, R. Cava, S. Kivelson, D. Nocera, M. Norman, and T. Senthil, Science **367** (2020).
[4] P. W. Anderson, Mater. Res. Bull. **8**, 153 (1973).

[5] S. M. Winter, A. A. Tsirlin, M. Daghofer, J. van den Brink, Y. Singh, P. Gegenwart, and R. Valentí, J. Phys. Condens. Matter **29**, 493002 (2017).
[6] H. Takagi, T. Takayama, G. Jackeli, G. Khaliullin, and S. E. Nagler, Nat. Rev. Phys. **1**, 264 (2019).
[7] Y. Motome and J. Nasu, J. Phys. Soc. Jpn. **89**, 012002 (2020).
[8] S. Trebst and C. Hickey, Phys. Rep. **950**, 1 (2022).
[9] A. Kitaev, Ann. Phys. (Amsterdam) **321**, 2 (2006).
[10] G. Jackeli and G. Khaliullin, Phys. Rev. Lett. **102**, 017205 (2009).
[11] K. W. Plumb, J. P. Clancy, L. J. Sandilands, V. V. Shankar, Y. F. Hu, K. S. Burch, H.-Y. Kee, and Y.-J. Kim, Phys. Rev. B **90**, 041112(R) (2014).
[12] J. Chaloupka, G. Jackeli, and G. Khaliullin, Phys. Rev. Lett. **105**, 027204 (2010).
[13] Y. Singh and P. Gegenwart, Phys. Rev. B **82**, 064412 (2010).
[14] A. Banerjee, C. Bridges, J.-Q. Yan, A. Aczel, L. Li, M. Stone, G. Granroth, M. Lumsden, Y. Yiu, J. Knolle, S. Bhattacharjee, D. L. Kovrizhin, R. Moessner, D. Tennant, D. Mandrus, and S. Nagler, Nat. Mater. **15**, 733 (2016).
[15] A. Banerjee, J. Yan, J. Knolle, C. A. Bridges, M. B. Stone, M. D. Lumsden, D. G. Mandrus, D. A. Tennant, R. Moessner, and S. E. Nagler, Science **356**, 1055 (2017).
[16] S. H. Chun, J.-W. Kim, J. Kim, H. Zheng, C. C. Stoumpos, C. D. Malliakas, J. F. Mitchell, K. Mehlawat, Y. Singh, Y. Choi, T. Gog, A. Al-Zein, M. Moretti Sala, M. Krisch, J. Chaloupka, G. Jackeli, G. Khaliullin, and B. J. Kim, Nat. Phys. **11**, 462 (2015).
[17] J. Kim, J. Chaloupka, Y. Singh, J. W. Kim, B. J. Kim, D. Casa, A. Said, X. Huang, and T. Gog, Phys. Rev. X **10**, 021034 (2020).
[18] J. Chaloupka, G. Jackeli, and G. Khaliullin, Phys. Rev. Lett. **110**, 097204 (2013).
[19] V. M. Katukuri, S. Nishimoto, V. Yushankhai, A. Stoyanova, H. Kandpal, S. Choi, R. Coldea, I. Rousochatzakis, L. Hozoi, and J. van den Brink, New J. Phys. **16**, 013056 (2014).
[20] J. G. Rau, Eric Kin-Ho Lee, and H.-Y. Kee, Phys. Rev. Lett. **112**, 077204 (2014).
[21] J. A. Sears, Y. Zhao, Z. Xu, J. W. Lynn, and Y.-J. Kim, Phys. Rev. B **95**, 180411(R) (2017).
[22] Y. Kasahara, T. Ohnishi, Y. Mizukami, O. Tanaka, S. Ma, K. Sugii, N. Kurita, H. Tanaka, J. Nasu, Y. Motome, T. Shibauchi, and Y. Matsuda, Nature (London) **559**, 227 (2018).
[23] A. Banerjee, P. Lampen-Kelley, J. Knolle, C. Balz, A. A. Aczel, B. Winn, Y. Liu, D. Pajerowski, J. Yan, C. A. Bridges, A. T. Savici, B. C. Chakoumakos, M. D. Lumsden, D. A. Tennant, R. Moessner, D. G. Mandrus, and S. E. Nagler, npj Quantum Mater. **3**, 8 (2018).
[24] T. Yokoi, S. Ma, Y. Kasahara, S. Kasahara, T. Shibauchi, N. Kurita, H. Tanaka, J. Nasu, Y. Motome, C. Hickey, S. Trebst, and Y. Matsuda, Science **373**, 568 (2021).
[25] O. Tanaka, Y. Mizukami, R. Harasawa, K. Hashimoto, K. Hwang, N. Kurita, H. Tanaka, S. Fujimoto, Y. Matsuda, E.-G. Moon, and T. Shibauchi, Nat. Phys. **18**, 429 (2022).
[26] H. Liu and G. Khaliullin, Phys. Rev. B **97**, 014407 (2018).
[27] R. Sano, Y. Kato, and Y. Motome, Phys. Rev. B **97**, 014408 (2018).
[28] H. Liu, J. Chaloupka, and G. Khaliullin, Phys. Rev. Lett. **125**, 047201 (2020).
[29] Y. Motome, R. Sano, S. Jang, Y. Sugita, and Y. Kato, J. Phys. Condens. Matter **32**, 404001 (2020).
[30] C. Kim, H.-S. Kim, and J.-G. Park, J. Phys. Condens. Matter **34**, 023001 (2022).
[31] H. Liu, Int. J. Mod. Phys. B **35**, 2130006 (2021).
[32] L. Viciu, Q. Huang, E. Morosan, H. Zandbergen, N. Greenbaum, T. McQueen, and R. Cava, J. Solid State Chem. **180**, 1060 (2007).
[33] E. Lefrançois, M. Songvilay, J. Robert, G. Nataf, E. Jordan, L. Chaix, C. V. Colin, P. Lejay, A. Hadj-Azzem, R. Ballou, and V. Simonet, Phys. Rev. B **94**, 214416 (2016).
[34] A. K. Bera, S. M. Yusuf, A. Kumar, and C. Ritter, Phys. Rev. B **95**, 094424 (2017).
[35] G. Xiao, Z. Xia, W. Zhang, X. Yue, S. Huang, X. Zhang, F. Yang, Y. Song, M. Wei, H. Deng, and D. Jiang, Cryst. Growth Des. **19**, 2658 (2019).
[36] M. I. Stratan, I. L. Shukaev, T. M. Vasilchikova, A. N. Vasiliev, A. N. Korshunov, A. I. Kurbakov, V. B. Nalbandyan, and E. A. Zvereva, New J. Chem. **43**, 13545 (2019).
[37] C. Wong, M. Avdeev, and C. D. Ling, J. Solid State Chem. **243**, 18 (2016).
[38] J.-Q. Yan, S. Okamoto, Y. Wu, Q. Zheng, H. D. Zhou, H. B. Cao, and M. A. McGuire, Phys. Rev. Mater. **3**, 074405 (2019).
[39] E. Zvereva, M. Stratan, A. Ushakov, V. Nalbandyan, I. Shukaev, c. V. Silhanek, M. Abdel-Hafiez, S. Streltsov, and A. Vasiliev, Dalton Trans. **45**, 7373 (2016).
[40] Y. Ishikawa and S.-i. Akimoto, J. Phys. Soc. Jpn. **13**, 1298 (1958).
[41] B. Yuan, I. Khait, G.-J. Shu, F. C. Chou, M. B. Stone, J. P. Clancy, A. Paramekanti, and Y.-J. Kim, Phys. Rev. X **10**, 011062 (2020).
[42] L. Regnault, P. Burlet, and J. Rossat-Mignod, Physica (Amsterdam) **86B+C**, 660 (1977).
[43] R. Zhong, T. Gao, N. P. Ong, and R. J. Cava, Sci. Adv. **6**, eaay6953 (2020).
[44] H. S. Nair, J. M. Brown, E. Coldren, G. Hester, M. P. Gelfand, A. Podlesnyak, Q. Huang, and K. A. Ross, Phys. Rev. B **97**, 134409 (2018).
[45] W. Yao and Y. Li, Phys. Rev. B **101**, 085120 (2020).
[46] G. Lin *et al.*, Nat. Commun. **12**, 5559 (2021).
[47] X. Hong, M. Gillig, R. Hentrich, W. Yao, V. Kocsis, A. R. Witte, T. Schreiner, D. Baumann, N. Pérez, A. U. B. Wolter, Y. Li, B. Büchner, and C. Hess, Phys. Rev. B **104**, 144426 (2021).
[48] M. Songvilay, J. Robert, S. Petit, J. A. Rodriguez-Rivera, W. D. Ratcliff, F. Damay, V. Balédent, M. Jiménez-Ruiz, P. Lejay, E. Pachoud, A. Hadj-Azzem, V. Simonet, and C. Stock, Phys. Rev. B **102**, 224429 (2020).
[49] W. Chen, X. Li, Z. Hu, Z. Hu, L. Yue, R. Sutarto, F. He, K. Iida, K. Kamazawa, W. Yu, X. Lin, and Y. Li, Phys. Rev. B **103**, L180404 (2021).
[50] A. M. Samarakoon, Q. Chen, H. Zhou, and V. O. Garlea, Phys. Rev. B **104**, 184415 (2021).

[51] C. Kim, J. Jeong, G. Lin, P. Park, T. Masuda, S. Asai, S. Itoh, H.-S. Kim, H. Zhou, J. Ma, and J.-G. Park, J. Phys. Condens. Matter **34**, 045802 (2022).

[52] A. L. Sanders, R. A. Mole, J. Liu, A. J. Brown, D. Yu, C. D. Ling, and S. Rachel, Phys. Rev. B **106**, 014413 (2022).

[53] L. Janssen, E. C. Andrade, and M. Vojta, Phys. Rev. Lett. **117**, 277202 (2016).

[54] K. Momma and F. Izumi, J. Appl. Crystallogr. **44**, 1272 (2011).

[55] See Supplemental Material at http://link.aps.org/supplemental/10.1103/PhysRevLett.129.147202 for additional methods, data, and analyses, which includes additional Refs. [56,57].

[56] P. Fazekas, *Lecture Notes on Electron Correlation and Magnetism* (World Scientific, Singapore, 1999), Vol. 5.

[57] E. Rastelli, A. Tassi, and L. Reatto, Physica (Amsterdam) **97B+C**, 1 (1979).

[58] R. Kajimoto *et al.*, J. Phys. Soc. Jpn. **80**, SB025 (2011).

[59] M. Nakamura, R. Kajimoto, Y. Inamura, F. Mizuno, M. Fujita, T. Yokoo, and M. Arai, J. Phys. Soc. Jpn. **78**, 093002 (2009).

[60] Y. Inamura, T. Nakatani, J. Suzuki, and T. Otomo, J. Phys. Soc. Jpn. **82**, SA031 (2013).

[61] R. Ewings, A. Buts, M. Le, J. Van Duijn, I. Bustinduy, and T. Perring, Nucl. Instrum. Methods Phys. Res., Sect. A **834**, 132 (2016).

[62] R. T. Azuah, L. R. Kneller, Y. Qiu, P. L. Tregenna-Piggott, C. M. Brown, J. R. Copley, and R. M. Dimeo, J. Res. Natl. Inst. Stand. Technol. **114**, 341 (2009).

[63] G. Xu, Z. Xu, and J. Tranquada, Rev. Sci. Instrum. **84**, 083906 (2013).

[64] S. Toth and B. Lake, J. Phys. Condens. Matter **27**, 166002 (2015).

[65] H. B. Cao, A. Banerjee, J.-Q. Yan, C. A. Bridges, M. D. Lumsden, D. G. Mandrus, D. A. Tennant, B. C. Chakoumakos, and S. E. Nagler, Phys. Rev. B **93**, 134423 (2016).

[66] S. K. Choi, R. Coldea, A. N. Kolmogorov, T. Lancaster, I. I. Mazin, S. J. Blundell, P. G. Radaelli, Y. Singh, P. Gegenwart, K. R. Choi, S.-W. Cheong, P. J. Baker, C. Stock, and J. Taylor, Phys. Rev. Lett. **108**, 127204 (2012).

[67] C. Kim, J. Jeong, P. Park, T. Masuda, S. Asai, S. Itoh, H.-S. Kim, A. Wildes, and J.-G. Park, Phys. Rev. B **102**, 184429 (2020).

[68] W. J. L. Buyers, T. M. Holden, E. C. Svensson, R. A. Cowley, and M. T. Hutchings, J. Phys. C **4**, 2139 (1971).

[69] J. Lorenzana, G. Seibold, and R. Coldea, Phys. Rev. B **72**, 224511 (2005).

[70] J. Fouet, P. Sindzingre, and C. Lhuillier, Eur. Phys. J. B **20**, 241 (2001).

[71] J. Reuther, D. A. Abanin, and R. Thomale, Phys. Rev. B **84**, 014417 (2011).

[72] J. Chaloupka and G. Khaliullin, Phys. Rev. B **92**, 024413 (2015).

[73] L. Chen, J.-H. Chung, B. Gao, T. Chen, M. B. Stone, A. I. Kolesnikov, Q. Huang, and P. Dai, Phys. Rev. X **8**, 041028 (2018).

[74] B. Gao, T. Chen, C. Wang, L. Chen, R. Zhong, D. L. Abernathy, D. Xiao, and P. Dai, Phys. Rev. B **104**, 214432 (2021).

[75] A. Furrer and O. Waldmann, Rev. Mod. Phys. **85**, 367 (2013).

[76] Y. Sizyuk, C. Price, P. Wölfle, and N. B. Perkins, Phys. Rev. B **90**, 155126 (2014).

[77] S. M. Winter, Y. Li, H. O. Jeschke, and R. Valentí, Phys. Rev. B **93**, 214431 (2016).

[78] I. Kimchi and Y.-Z. You, Phys. Rev. B **84**, 180407(R) (2011).

[79] L. Messio, C. Lhuillier, and G. Misguich, Phys. Rev. B **83**, 184401 (2011).

[80] I. I. Mazin, H. O. Jeschke, K. Foyevtsova, R. Valentí, and D. I. Khomskii, Phys. Rev. Lett. **109**, 197201 (2012).

[81] K. Foyevtsova, H. O. Jeschke, I. I. Mazin, D. I. Khomskii, and R. Valentí, Phys. Rev. B **88**, 035107 (2013).

[82] L. Janssen, E. C. Andrade, and M. Vojta, Phys. Rev. B **96**, 064430 (2017).

[83] P. A. Maksimov and A. L. Chernyshev, Phys. Rev. Res. **2**, 033011 (2020).

[84] P. Laurell and S. Okamoto, npj Quantum Mater. **5**, 2 (2020).

[85] S.-H. Do, S.-Y. Park, J. Yoshitake, J. Nasu, Y. Motome, Y. S. Kwon, D. Adroja, D. Voneshen, K. Kim, T.-H. Jang, J.-H. Park, K.-Y. Choi, and S. Ji, Nat. Phys. **13**, 1079 (2017).

[86] J. R. Morey, A. Scheie, J. P. Sheckelton, C. M. Brown, and T. M. McQueen, Phys. Rev. Mater. **3**, 014410 (2019).

[87] C. L. Sarkis, J. G. Rau, L. D. Sanjeewa, M. Powell, J. Kolis, J. Marbey, S. Hill, J. A. Rodriguez-Rivera, H. S. Nair, D. R. Yahne, S. Säubert, M. J. P. Gingras, and K. A. Ross, Phys. Rev. B **102**, 134418 (2020).

[88] S.-H. Lee, C. Broholm, W. Ratcliff, G. Gasparovic, Q. Huang, T. Kim, and S.-W. Cheong, Nature (London) **418**, 856 (2002).

[89] K. Tomiyasu, H. Suzuki, M. Toki, S. Itoh, M. Matsuura, N. Aso, and K. Yamada, Phys. Rev. Lett. **101**, 177401 (2008).

[90] K. Tomiyasu, H. Ueda, M. Matsuda, M. Yokoyama, K. Iwasa, and K. Yamada, Phys. Rev. B **84**, 035115 (2011).

[91] K. Tomiyasu, M. K. Crawford, D. T. Adroja, P. Manuel, A. Tominaga, S. Hara, H. Sato, T. Watanabe, S. I. Ikeda, J. W. Lynn, K. Iwasa, and K. Yamada, Phys. Rev. B **84**, 054405 (2011).

[92] S. Janas, J. Lass, A.-E. Ţuţueanu, M. L. Haubro, C. Niedermayer, U. Stuhr, G. Xu, D. Prabhakaran, P. P. Deen, S. Holm-Dahlin, and K. Lefmann, Phys. Rev. Lett. **126**, 107203 (2021).